Experimental Confirmation of Impurity Convection Driven by the Ion-Temperature Gradient in Toroidal Plasmas

M. R. Wade, W. A. Houlberg, and L. R. Baylor
Oak Ridge National Laboratory, Oak Ridge, Tennessee 37831
(Received 9 February 1999)

Strong, outward convection of low-Z impurity ions has been observed in DIII-D plasmas which have reduced anomalous transport, a weak density gradient, and a strong ion-temperature gradient. Comparing the measurements with theoretical predictions of collisional (neoclassical) transport indicates that the observed outward convection results from an effect known as "temperature screening." Taking into account the non-negligible effect of anomalous transport, quantitative agreement is found between the measured transport properties and the predicted values, including the strong Z dependence.

PACS numbers: 52.55.Fa, 52.25.Fi, 52.25.Vy

Evidence of impurity "temperature screening," as predicted by neoclassical transport theory, has been observed for the first time on the DIII-D tokamak. The thermal force responsible for this screening effect arises from the strong velocity dependence ($\nu \sim v^{-3}$) of the Coulomb collision frequency [1]. In toroidal magnetized plasmas, the guiding-center drift [$v_{\mathrm{dr}} \propto (\vec{F} \times \vec{B})/B^2$] associated with this thermal force leads to impurity transport in the direction of the thermal gradient. The theory of collisional transport of energy and particles in toroidal confinement devices (so-called neoclassical transport) has been well established in magnetic fusion research since the early 1980s [2–6]. This theory predicts that in certain collisionality regimes the cross-field particle flux of higher charge and mass impurities would be directed down the main ion-temperature gradient, resulting in a phenomenon known as "temperature screening" [2]. In this Letter, we present experimental confirmation of this prediction.

Any clear experimental observation of temperature screening of impurities requires four conditions to be achieved *simultaneously:* (i) Turbulent transport must be reduced sufficiently such that the cross-field transport due to collisions constitutes a non-negligible portion of the total transport rate; (ii) the ion density gradient must be small; (iii) a strong ion-temperature gradient must be present; and (iv) the impurity of interest must be in the proper collisionality regime. In its most basic form, the neoclassical cross-field impurity flux is

$$\Gamma_z^{\mathrm{neoc}} = -D_z^{\mathrm{neoc}} \nabla n_z + D_z^{\mathrm{neoc}} n_z \times \left[\sum_{j \neq z} \left(g_{n_{j\to z}} \frac{\nabla n_j}{n_j} \right) + g_{T_i} \frac{\nabla T_i}{T_i} + g_{T_e} \frac{\nabla T_e}{T_e} \right], \quad (1)$$

where D_z^{neoc} is the neoclassical diffusion coefficient for impurity species of charge Z on its own density gradient, n_z is impurity density, n_j is the density of plasma species j, T_i and T_e are the ion and electron temperatures, and ∇ indicates the gradient in the cross-field direction. The parameters $g_{n_{j\to z}}$, g_{T_i}, g_{T_e} depend on the details of momentum transfer between the various particle species and are therefore dependent on local plasma conditions. Because momentum transfer between electrons and impurities is small, the terms $g_{n_{e\to z}}$ and g_{T_e} can generally be neglected in Eq. (1). Thus, for most cases of interest, Eq. (1) yields a steady-state (i.e., $\Gamma_z = 0$) impurity density profile of the form $n_z(\rho) = n_z(0)[n_D(\rho)/n_D(0)]^{g_{n_{D\to z}}}[T_i(\rho)/T_i(0)]^{g_{T_i}}$. Generally, $g_{n_{D\to z}} \gg g_{T_i}$. Hence, in plasmas with a peaked main ion density profile, impurities would be expected to concentrate in the plasma center regardless of the ion-temperature profile. The validity of this prediction has been confirmed in experiments with strong central fueling either by pellet injection [7] or neutral beam fueling [8]. In these cases, peaked main ion density profiles are produced and are accompanied by central accumulation of both low-Z and high-Z impurities. However, in cases in which the ion density gradient is small, the impurity flux driven by the ion-temperature gradient does become important.

Since g_{T_i} is a complex function of both the main ion collisionality ν_{*_i} and the impurity collisionality ν_{*_Z}, the ion-temperature-gradient driven flux is a complicated function of plasma conditions. Here, ν_* is defined as $\nu_* = \nu R q / v_{\mathrm{th}} \varepsilon^{3/2}$, where ν is the collision frequency, R is the plasma major radius, q is the plasma safety factor, v_{th} is the thermal velocity, and $\varepsilon = r/R_0$ is the inverse aspect ratio. For tokamak plasmas of interest, the main ions are generally deep in the long-mean free path regime [i.e., "banana" regime ($\nu_{*_i} < 1$)]. If the impurity of interest is also in the banana regime, then the sign of g_{T_i} is generally negative, implying screening of the impurities.

In DIII-D very high confinement mode (VH mode) plasmas [9], all four conditions outlined above are met simultaneously. The time evolution of a typical VH-mode discharge is shown in Fig. 1. The early low-power phase is characterized by large levels of turbulence-driven transport with relatively poor energy and particle confinement and is hence called L mode (for low confinement). In these turbulence-dominated plasmas, the electron density and low-Z impurity density profiles are

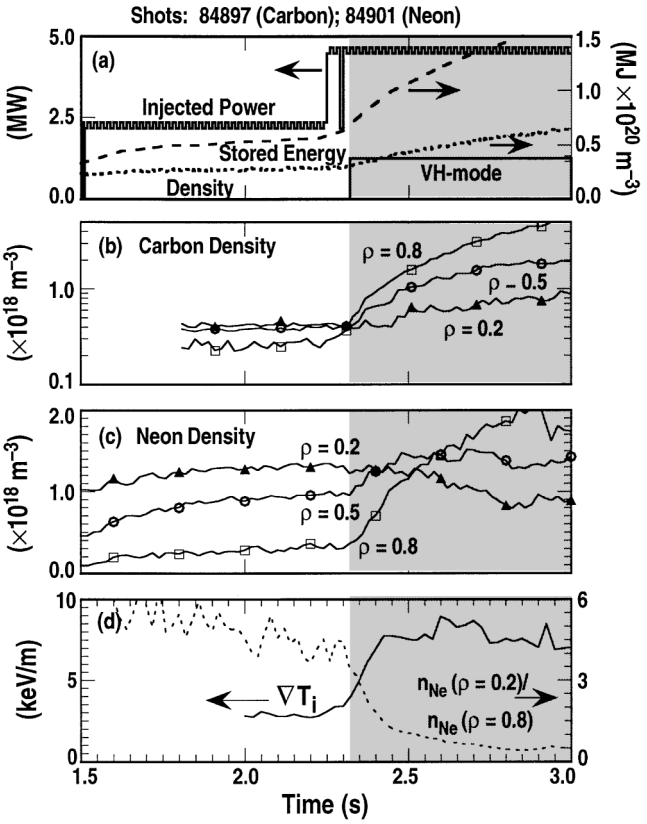

FIG. 1. Temporal evolution of the (a) line-averaged density (dotted), stored energy (dashed), and input power (solid); (b) carbon and (c) neon density at various radial locations and (d) ion temperature gradient at $\rho = 0.35$ (solid) and neon density peaking factor (dotted) in a VH-mode plasma in DIII-D.

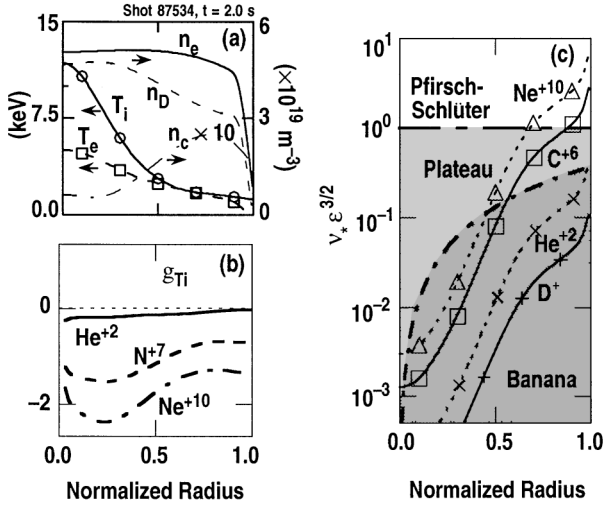

FIG. 2. Radial profiles of (a) ion temperature T_i, electron temperature T_e, electron density n_e, deuteron density n_D, and carbon density n_C; (b) the parameter g_{T_i} defined in Eq. (1), and (c) the main ion and impurity collisionalities measured approximately 500 ms after the initiation of the VH-mode phase of the discharge used for this study.

observed to have roughly the same shape, regardless of impurity charge or mass [10]. Furthermore, the electron diffusivity D_e, the low-Z impurity diffusivities D_z, and the single-fluid thermal diffusivity χ_{eff} have similar radial profiles and are comparable in magnitude (i.e., $D_e \approx D_z \approx \chi_{\text{eff}}$) [11,12].

Upon the initiation of the high power phase at 2.2 s, a rapid improvement in plasma confinement is observed coincident with a large reduction in turbulence in the outer half of the plasma [13]. At the beginning of the VH-mode phase, the electron density profile rapidly evolves from peaked to flat while a strong ion-temperature gradient forms in the plasma core due to central heating by neutral beam injection (Fig. 2), resulting in low collisionality in the plasma core. Hence, the four conditions outlined above are met simultaneously during the VH-mode phase. The response of the impurity density profiles, inferred from charge-exchange recombination (CER) spectroscopy [14] measurements, subsequent to the initiation of this VH-mode phase (Fig. 1) provides clear evidence that a strong outward convective component of the impurity particle flux is present. In this discharge, both the carbon and neon density profiles are observed to quickly reorganize from a centrally peaked profile to a strongly hollow profile during the VH-mode phase [Figs. 1(b) through 1(c)]. In DIII-D, carbon is the primary intrinsic impurity while neon was intentionally introduced into this discharge for diagnostic purposes. It should be noted that the inference of the impurity density profile relies on the accurate computation of the attenuation of the neutral beam due to ionization of the beam neutrals passing through the core plasma. As in previous studies [15], the accuracy of this calculation has been verified using independent measurements of the D_α emission from the neutral beam using the DIII-D motional Stark effect system. Care must also be taken in interpreting the impurity density as measured by CER as recent theoretical studies suggest that such a measurement may systematically overestimate the flux-surface-averaged impurity density in plasmas with strong toroidal rotation [16]. However, the corrections for the impurities of interest (namely, carbon and neon) are found to be modest ($<30\%$) because of the low Z of these impurities, and the degree of hollowness inferred from the measurements cannot be fully attributable to this effect.

The impurity particle flux can be described in most general terms as a sum of diffusive and convective components: $\Gamma_z = -D_z \nabla n_z + V_z n_z$, where D_z is the impurity diffusivity, and V_z is the impurity convective velocity. In the case of the carbon density profile evolution in Fig. 1, it is difficult from first principles to determine whether the progressively hollow profiles result from a strong outward convective component or from a strong carbon source at the edge of the plasma coupled with extremely low diffusivity in the core plasma, which, transiently, would result in a hollow profile. More convincing evidence is provided by the evolution of the neon density in the plasma center [Fig. 1(c)]. In this case, the neon density profile rapidly evolves

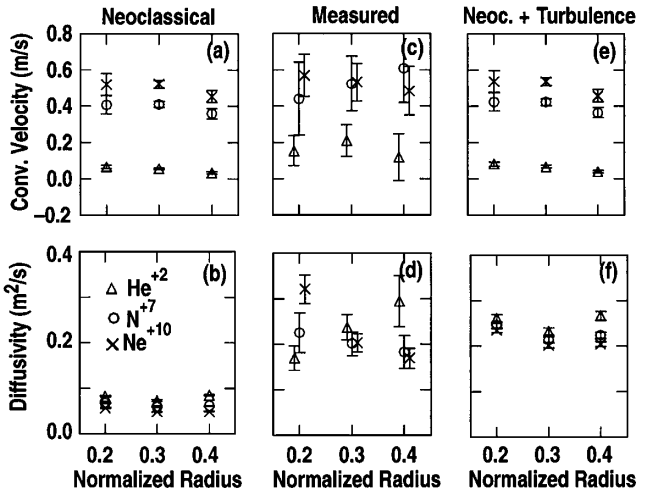

FIG. 3. Neoclassical predictions (a), (b), experimental measured values (c), (d), and predictions combining neoclassical and turbulence-driven flux (e), (f) for the convective velocity and diffusivity for the plasma conditions of Fig. 2(a). The error bars in the theoretical predictions are based on the uncertainties in the profile fitting of the measured data. Uncertainties based on local analysis of gradients rather than fitted profiles give a larger uncertainty in the convective velocity with $\sigma_{V_{\mathrm{He}}} \approx 0.015$ m/s, $\sigma_{V_{\mathrm{N}}} \approx 0.1$ m/s, and $\sigma_{V_{\mathrm{Ne}}} \approx 0.12$ m/s.

from peaked to hollow, with the central neon density decreasing by 33% during the VH-mode phase, which is much larger than the total systematic error ($\sim$10%) associated with the CER measurement and the beam attenuation calculation required to deduce the impurity density. This observation can be described only by an outward convective component of the neon particle flux acting to drive particles out of the plasma center.

To provide a more rigorous test of the neoclassical predictions, an experiment has been carried out to measure the transport coefficients of a variety of low-Z impurities in a reproducible set of VH-mode discharges. The plasma conditions chosen for this experiment were plasma current $I_p = 1.3$ MA, toroidal field $B_T = -2.1$ T, and injected power $P_{\mathrm{inj}} = 7.0$ MW with double-null diverted magnetic configuration. The VH-mode phase in this case lasted $\sim$800 ms, allowing sufficient time for the transport measurement. At 400 ms after the initiation of the VH-mode phase (i.e., 200 ms after the impurity gas injection), the electron and ion density profile (calculated from n_e and n_{C}) are flat while the ion and electron temperatures peak strongly on axis [Fig. 2(a)]. Deuterium and helium ions are well into the banana collisionality regime over the entire radius while carbon and neon are in the banana collisionality regime in the inner half of the plasma [Fig. 2(c)]. The parameter g_{T_i} is negative for all impurities [Fig. 2(b)].

The neoclassical theory predictions for this case, calculated with the NCLASS code [17], are shown in Figs. 3(a) and 3(b). This code takes as input experimentally measured profiles of electron density, electron and ion temperature, impurity density (Fig. 2), and toroidal rotation as well as the magnetic equilibrium computed by the EFIT magnetic reconstruction code [18]. Although the impurity density profile of each introduced impurity should be included in this calculation as collisions between different species affect transport, we have included only the carbon density profile since the remainder of the impurities were introduced at the trace level. The uncertainties in the theoretical prediction are estimated by varying the measured plasma profiles by their standard deviations, computing the best fit to the obtained profile, and then recalculating the neoclassical transport coefficients; the resulting uncertainties are then combined in quadrature assuming that the errors are uncorrelated. For the experimental profiles shown in Fig. 2(a), the theory predicts a strong Z dependence of the convective velocity while the diffusivity is only weakly dependent on impurity species. The various components of the convective flux at a normalized radius $\rho = 0.3$ are tabulated in Table I. As expected, the convective fluxes resulting from the ion density and temperature gradients are the major contributors to the total convective flux, and both of these contributions have a strong Z dependence. The plasma conditions in this case (i.e., a strong ion temperature gradient and a weak deuteron density gradient) lead to a net outward flux of nitrogen and neon while the helium flux is nearly zero. This strong Z dependence in the theory results from the nonlinear variation in the momentum exchange between the deuterons and the impurity ions as the charge and mass are increased.

Experimentally, the local impurity transport coefficients (D_z and V_z) are determined by linear regression of the inferred impurity particle flux Γ_z and the measured impurity density gradient subsequent to a nonperturbative impurity gas puff, assuming the impurity flux takes on the general form given above. Here, Γ_z is determined from the impurity continuity equation: $dn_z/dt = -\nabla \cdot \Gamma_z$ [11,19]. In computing the uncertainties in the integrals that are required for the determination of Γ_z, the statistical error is propagated assuming that the errors are uncorrelated. Finally, both the errors in the normalized density gradient ($\nabla n_z/n_z$) and the normalized flux (Γ_z/n_z) are included in the linear regression analysis to determine D_z and V_z and their uncertainties. Because of diagnostic constraints, the radial region over which this method is accurate is limited.

TABLE I. NCLASS prediction of the contributions from the various components of the convective velocity for the plasma conditions of Fig. 2(a).

V_z due to: (m/s)	He^{+2}	N^{+7}	Ne^{+10}
$\nabla T_e/T_e$	0.0	0.0	0.0
$\nabla T_i/T_i$	0.065	0.44	0.55
$\nabla n_e/n_e$	0.0	0.0	0.0
$\nabla n_D/n_D$	−0.06	−0.17	−0.20
$\nabla n_c/n_c$	0.06	0.19	0.24
Total	0.064	0.46	0.58

The inferred values of convective velocity are found to be in good agreement with the theoretical predictions including the strong increase with impurity charge [Fig. 3(c)]. As in the theoretical case, the measured values of diffusivity vary weakly with impurity species [Fig. 3(d)]; however, the impurity diffusivity is found to be a factor of 2–4 larger than the theoretical predictions.

Because the total transport rate still retains a component due to turbulence-driven radial transport in these plasmas, the observation of enhanced impurity diffusivity relative to the neoclassically predicted value is expected. Unfortunately, there is no experimental method through which the collision-driven and turbulence-driven fluxes can be decoupled. However, one can estimate the variations from neoclassical theory that might be expected due to turbulence-driven transport. Invoking the argument of Fussman *et al.* [20] that the large-scale characteristics of the fluctuation-induced transport should not affect momentum exchange between the various species, the measured impurity flux can be decomposed into a collision-driven (i.e., neoclassical) flux and a turbulence-driven flux: $\Gamma_z = \Gamma_z^{\text{neoc}} + \Gamma_z^{\text{turb}} = -(D_z^{\text{neoc}} + D_z^{\text{turb}})\nabla n_z + (V_z^{\text{neoc}} + V_z^{\text{turb}})n_z$. In the following, the relative importance of collisional versus collective processes is parametrized using the parameter $\xi = D_z^{\text{neoc}}/D_z^{\text{turb}}$.

To make this estimate, the following assumptions are required: (i) $D_z^{\text{turb}} = \chi_{\text{eff}}^{\text{turb}}$; (ii) $V_z^{\text{turb}}/D_z^{\text{turb}} = V_e^{\text{turb}}/D_e^{\text{turb}}$; and (iii) total electron transport is dominated by turbulence-driven transport (i.e., $D_e = D_e^{\text{turb}}$, $V_e = V_e^{\text{turb}}$). The first two of these assumptions have been discussed earlier. The final assumption is supported by transport analysis which shows the electron transport rates in these VH-mode plasmas to be $\sim 10-20$ times that expected from collisions alone. Using these assumptions, $\xi = D_z^{\text{neoc}}/\chi_{\text{eff}}^{\text{turb}} \approx D_z^{\text{neoc}}/\chi_{\text{eff}}^{\text{meas}}$ and $V_z^{\text{turb}}/D_z^{\text{turb}} \approx \nabla n_e/n_e$, provided that the electron density profile in the core region is not strongly influenced by neutral beam fueling [i.e., $\nabla n_e/n_e > (S_e - dN_e/dt)/n_e D_e^{\text{turb}} A$, where S_e is the volume-integrated electron source rate from neutral beam fueling, N_e is the volume-integrated electron density, and A is the surface area at the flux surface of interest]. Transport analysis indicates that this provision is met in this case with $|\nabla n_e/n_e| \approx 0.15\ \text{m}^{-1}$ and $(S_e - dN_e/dt)/n_e D_e^{\text{turb}} A \approx 0.05\ \text{m}^{-1}$. These parametrizations allow the total diffusivity and convective velocity to be written as $D_Z^{\text{tot}} = D_Z^{\text{neoc}}(1 + \xi^{-1})$ and $V_z^{\text{tot}} \approx V_z^{\text{neoc}} + D_z^{\text{neoc}}\xi^{-1}\nabla n_e/n_e$. This formulation thus predicts that D_z^{tot} will be sensitive to the value of ξ while V_z^{tot} will only vary weakly with ξ when $\nabla n_e/n_e \approx 0$. The predicted diffusivity and convective velocity based on this set of assumptions are shown in Figs. 3(e) and 3(f). The primary result is that the "theoretically expected" diffusivities rise significantly while the convective velocities are unaffected, resulting in a prediction that is in quantitative agreement with the measured values.

In conclusion, a strong, outward convection of low-Z impurities has been observed in VH-mode plasmas in the DIII-D tokamak with the magnitude of the convection increasing strongly with impurity charge. Quantitative agreement is found over a moderate range in impurity charge between experimental measurements of the convective velocity and the theoretically predicted values. According to the theory, this outward convective flux is dominated by convection driven by the ion-temperature-gradient driven flux (or temperature screening). Calculations based on these findings suggest that this temperature screening effect will have a favorable impact on the impurity density distribution in a reactor device such as ITER even when turbulence-driven transport dominates the total transport rate [21]. Because temperature screening is not predicted to have a substantial impact on helium transport, it is expected that helium ash removal will be neither benefited nor deterred by this process.

This is a report of work supported by the U.S. Department of Energy under Contracts No. DE-AC05-96OR22464 and No. DE-AC03-99ER54463.

[1] S. I. Braginskii, in *Reviews of Plasma Physics*, edited by M. A. Leontovich (Consultants Bureau, New York, 1965), Vol. 1, p. 205.
[2] P. H. Rutherford, Phys. Fluids **17**, 1782 (1974).
[3] F. L. Hinton and T. B. Moore, Nucl. Fusion **14**, 639 (1974).
[4] S. P. Hirshman, D. J. Sigmar, and J. F. Clarke, Phys. Fluids **19**, 656 (1976).
[5] S. P. Hirshman and D. J. Sigmar, Nucl. Fusion **21**, 1079 (1981).
[6] C. L. Longmire and M. N. Rosenbluth, Phys. Rev. **103**, 507 (1956).
[7] S. L. Milora *et al.*, Nucl. Fusion **35**, 657 (1995).
[8] E. J. Snyakowski *et al.*, Phys. Fluids B **5**, 2215 (1993).
[9] G. L. Jackson *et al.*, Phys. Rev. Lett. **67**, 3098 (1991).
[10] M. R. Wade *et al.*, in *Proceedings of the 23rd EPS Conference on Controlled Fusion and Plasma Physics, Kiev, Russia, 1996* (European Physical Society, 1997), Vol. 1, p. 283.
[11] M. R. Wade *et al.*, Phys. Plasmas **2**, 2357 (1995).
[12] D. R. Baker *et al.*, Nucl. Fusion **38**, 485 (1998).
[13] T. H. Osborne *et al.*, Nucl. Fusion **35**, 23 (1995).
[14] P. Gohil *et al.*, in *Proceedings of the 14th Symposium on Fusion Engineering, San Diego, California, 1992* (Institute of Electronics and Electrical Engineers, Inc., Piscataway, New Jersey, 1993), Vol. 2, p. 1199.
[15] D. G. Whyte *et al.*, Nucl. Fusion **38**, 387 (1998).
[16] J. A. Wesson Nucl. Fusion **5**, 577 (1997).
[17] W. A. Houlberg *et al.*, Phys. Plasmas **4**, 3281 (1997).
[18] L. L. Lao *et al.*, Nucl. Fusion **30**, 1035 (1990).
[19] M. R. Wade, T. C. Luce, and C. C. Petty, Phys. Rev. Lett. **79**, 419 (1997).
[20] G. Fussmann *et al.*, Plasma Phys. Controlled Fusion **33**, 1677 (1991).
[21] W. A. Houlberg and L. R. Baylor, Fusion Technol. **34**, 591 (1998).